NANO LETTERS

Letter

pubs.acs.org/NanoLett

High-Frequency Mechanical Stirring Initiates Anisotropic Growth of Seeds Requisite for Synthesis of Asymmetric Metallic Nanoparticles like Silver Nanorods

Mahmoud A. Mahmoud,[†] Mostafa A. El-Sayed,*[,†] Jianping Gao,[‡] and Uzi Landman[‡]

[†]Laser Dynamics Laboratory, School of Chemistry and Biochemistry, Georgia Institute of Technology, Atlanta, Georgia 30332-0400, United States

[‡]School of Physics, Georgia Institute of Technology, Atlanta, Georgia 30332-0430, United States

Supporting Information

ABSTRACT: High-speed stirring at elevated temperatures is shown to be effective in the symmetry-breaking process needed for the growth of the hard-to-synthesize silver nanorods from the polyol reduction of silver ions. This process competes with the facile formation of more symmetrical, spherical and cubic, nanoparticles. Once the seed is formed, further growth proceeds predominantly along the long axis, with a consequent increase of the particles' aspect ratio (that of the nanorod). When stirring is stopped shortly after seed formation, nanorods with a broad distribution of aspect ratios are obtained, while when the high-frequency stirring continues the distribution narrows significantly. The width of the nanorods can only be increased if the initial concentration of Ag^+ ions increases. Reducing the stirring speeds during seed formation lowers the yield of nanorods. Molecular dynamics simulations reveal that the formation of a nanometer-scale thin boundary region between a solid facet of the nanoparticle and the liquid around it, and the accommodation processes of metal (Ag) atoms transported through this boundary region from the liquid to the solid growth interface, are frustrated by sufficiently fast shear flow caused by high-frequency stirring. This arrests growth on seed facets parallel to the flow, leading, together with the preferential binding of the capping polymer to the (100) facet, to the observed growth in the (110) direction, resulting in silver nanorods capped at the ends by (111) facets and exposing (100) facets on the side walls.

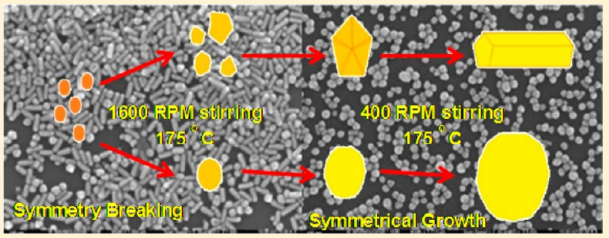

KEYWORDS: *Silver, growth, symmetry breaking, twinning, nanorods, high-frequency stirring*

The optical, chemical, mechanical, and physical properties of plasmonic nanoparticles depend on their shapes, sizes, and the medium dielectric function.[1,2] Colloidal chemical methods are the most common techniques used to synthesize nanoparticles.[2,3] One of the most important factors in these techniques pertains to the controlled synthesis of nanoparticles with a specific shape and size. In these methods, a small seed is formed which grows into a nanoparticle with a shape that depends on several factors.[4] These include: the shape of the seed, the relative rates of growth of the different facets of the crystalline cluster, and the stability of the different facets as influenced by the binding properties of the capping materials present in the growth solution.[5,6] Different synthetic protocols have been developed to prepare nanoparticles of symmetrical shapes such as spheres,[3] cubes,[7] octahedra, and prisms,[8,9] and asymmetrical shapes such as rods,[10−12] wires,[13,14] stars,[15,16] and so forth. Symmetrical shapes result from the growth of the low energy {100} and {111} facets, while asymmetric ones form when alternative routes set in, causing a crossover from growth along the {111} facet direction and the higher energy {110} one,[17] resulting in twinning. These asymmetric shapes can be obtained by symmetry breaking of the nancrystals' growth process. Physical,[18,19] chemical,[20] and optical[14] techniques have been utilized to bring about breaking the symmetry of the nanocrystals' growth mechanism by changing the balance between the growth propensities of the high and low energy facets energy facets, thus opening routes for fabrication of colloidal particles with more complex shapes. This can take place in a number of ways.

(1) The physical technique[18,19] of symmetry breaking of the nanocrystal growth is based on variation of the crystallization kinetics and the thermodynamic stability of the nanocrystals growing facets. These physical effects are controlled by varying the concentration of the silver precursor and the capping material used in the synthesis. Changing the molar ratio of the polyvinylpyrrolidone (PVP) capping agent and the silver ions during the polyol synthesis of silver nanoparticles changes the morphology of the final nanoparticle shape. Silver nanocubes are obtained when this molar concentration ratio is ~1.5 (the growth proceeds via formation of single crystalline seeds).[7] However, in the synthesis of silver nanowires, growth proceeds via the formation of pentatwinned seeds when this ratio is kept

Received: June 23, 2013
Revised: September 8, 2013
Published: September 20, 2013

   dx.doi.org/10.1021/nl402305n | *Nano Lett.* 2013, 13, 4739−4745

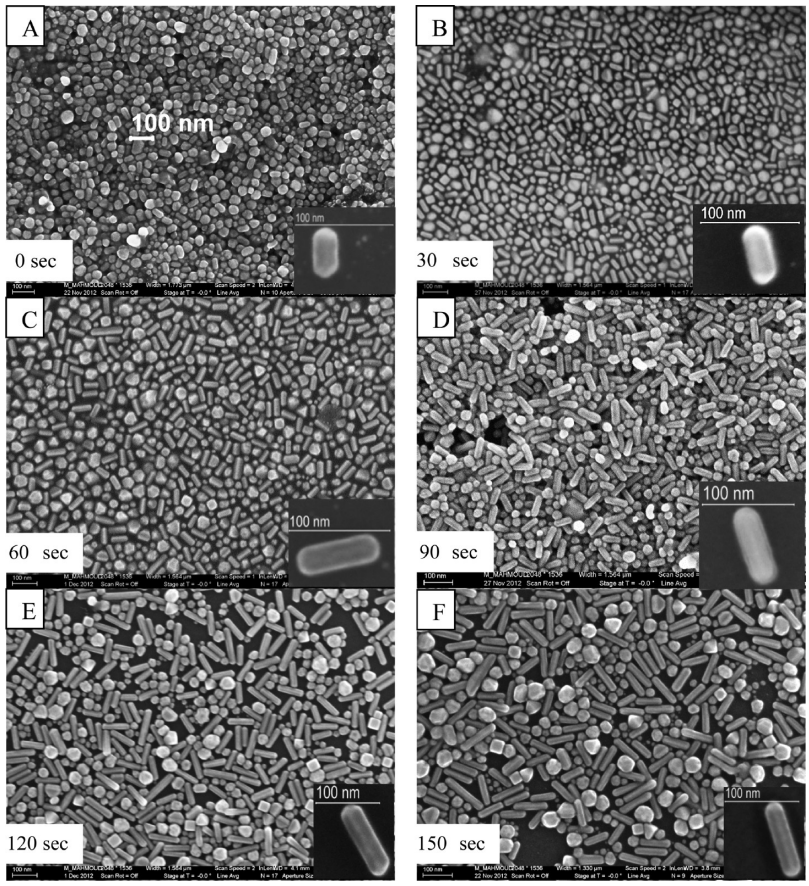

Figure 1. Time dependence of the growth of the different shapes of silver nanoparticles, in particular the nanorods, formed from the reduction of Ag^+ at 175 °C and stirring speed of 1600 rpm. (0 s is when the color of the solution becomes red.) Samples of nanoparticles are extracted from the growth solution at different reaction times from SEM images. It is clear that the length (and not the width) of the nanorods increases as the reduction time increases as follows: (A) 39.6 ± 3.2 nm, (B) 44.9 ± 4.7 nm, (C) 55.5 ± 5.5 nm, (D) 64.1 ± 5.6 nm, (E) 73.5 ± 7.8 nm, and (F) 86.0 ± 9.7 nm. The insets show the magnified images of single nanorods at different times during growth. The scale bars in all of the images are 100 nm.

constant at ∼1.5 for low concentrations of both silver ions and PVP. Quasi-spherical silver nanoparticles (that is, microfaceted aggregates with an overall approximate spherical shape) are formed when the PVP/silver ion molar ratio is increased to >5.[18] Manipulation of the reduction kinetics during the growth of the nanocrystals is an alternative physical technique for breaking the symmetry of the growth of the nanocrystals.[19]

(2) The growth symmetry can be broken by using a chemical method such as by the addition of silver ions in the synthesis of gold nanorods or by the introduction of chloride ions or oxygen to etch the defective seeds and drive the crystal growth to form single crystalline silver nanoparticles.[10,20]

(3) Pentatwinned seeds were obtained during the synthesis of silver nanoprisms due to breaking of the growth symmetry of the silver nanocrystals by light excitation.[14]

In this Letter we show that difficulties in synthesizing silver nanorods can be effectively overcome by rapid stirring at high temperatures during the reduction process of the silver ions (see Figure 1 and the experimental procedure in the Supporting Information). This suggests that mechanical action may be used as a new approach for breaking the growth symmetry. We note here that while stirring effects on the growth of single crystals from solutions and from the melt have been discussed in the past in a number of articles, starting from the early work of Nernst in 1904[21] and continuing up to the present,[22−25] it appears that the use of stirring as a way to control and direct the growth of asymmetrical crystalline shapes has not been explored previously. In this Letter, we studied experimentally and theoretically the effect of high speed stirring on shaping the asymmetric cluster needed for the growth of asymmetric crystalline nanoparticle like silver nanorods.

Results and Discussion. *Growth of Silver Nanorods at High Temperature and High Stirring Speeds.* Figure 1A−F shows the scanning electron microscopy (SEM) images of the nanoparticles formed with different reaction times from a solution mixture of 12.6 mM $AgNO_3$ and 64.3 mM of PVP in ethylene glycol at a stirring speed of 1600 rpm and 175 °C. The SEM images are of reaction mixture aliquots taken at different times. It is observed that the AgNRs get longer with increasing the reduction time. The length and diameter of the rods were determined by statistical analysis of 300 AgNRs per sample. The lengths, widths, and aspect ratios (ARs) of the AgNRs grown at increasing reduction time are given in Table S1 of the Supporting Information. It is clear that indeed the length of the nanorod (but not the width) changes during the growth process. A linear relationship is obtained between the length of the AgNRs and the growth time of the shortest observed AgNRs (see Figure S2). This can be taken as support of the idea that the growth of the nanorods is a first-order kinetic process. The inset of each SEM image shows that the AgNRs are of pentagonal cross-section, with side walls exposing low-energy (100) facets. This is similar to gold nanorods which

dx.doi.org/10.1021/nl402305n | *Nano Lett.* 2013, 13, 4739−4745

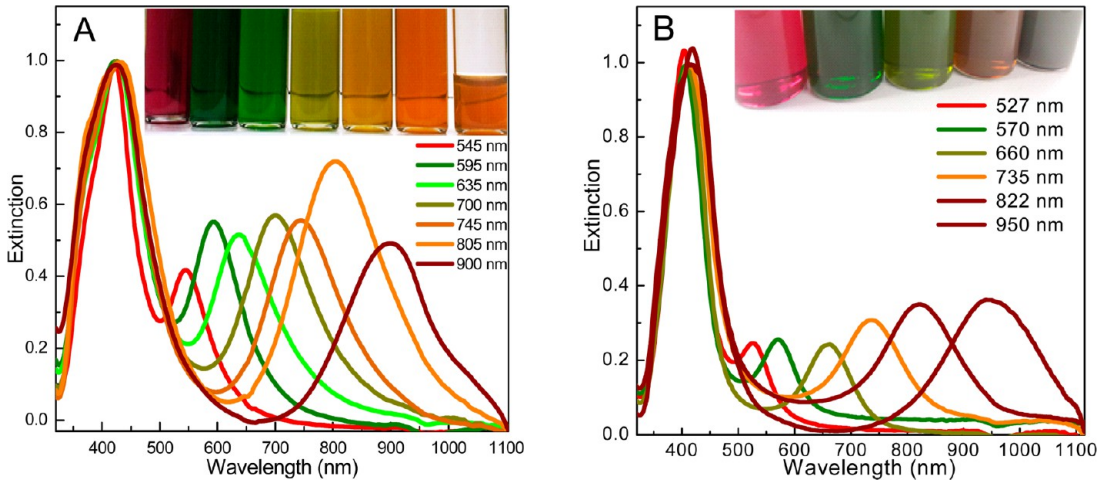

Figure 2. Dependence of the intensity of the longitudinal band of AgNR (which increases with increasing its length) formed at different growth times at 175 °C when two different stirring speeds are used: A: at 1600 rpm; B: at 1200 rpm.

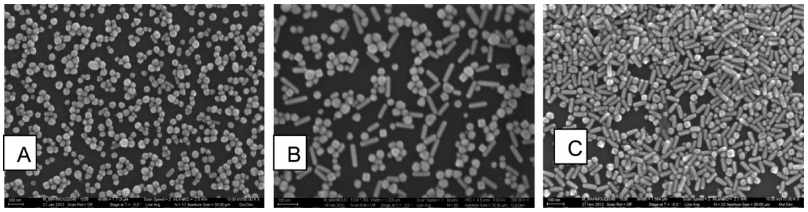

Figure 3. SEM images (of the same scale bars) of silver nanoparticles prepared at 175 °C and at different stirring speed: (A) At 400 rpm stirring no nanorods are formed. (B) At 1200 rpm the yield of AgNRs is low. (C) High-frequency stirring at 1600 rpm results in high-yield formation of AgNRs.

have been prepared as pentatwinned[26] and single crystalline[10] structures. High-resolution transmission electron microscopy (HR-TEM) was used to determine the exact face morphology of the AgNRs.

Silver nanorods and gold nanorods[10] are characterized by the presence of two localized surface plasmon resonance (LSPR) bands corresponding to the transverse (high energy) and longitudinal (low energy) modes of electronic oscillation.[27] The LSPR transverse peak position of AuNRs is usually at ~520 nm, while the position of the LSPR longitudinal peak depends on the nanorod's AR. During the synthesis of Ag or Au nanorods, spheres, and other shapes are also formed as shown in Figure 1, with characteristic plasmon extinctions that coincide with the transverse band of the Ag or Au nanorods. Thus the quality of any nanorod sample synthesis of a certain aspect ratio is determined by the ratio of the intensity of the band at the longitudinal band wavelength to that the transverse band wavelength. A high ratio is a good indication of the purity of the silver or the gold nanorods synthesized. Figure 2A shows the LSPR spectra of AgNRs with different ARs prepared at 1600 rpm stirring speed. The transverse LSPR peak is in the range of 400−450 nm, while the longitudinal LSPR peak shifts to longer wavelengths as the AR increases (Table S1) with increasing growth time.

Stirring Speed and Temperature Effects on the AgNR Synthesis. The LSPR spectrum of AgNRs prepared at a lower stirring speed (1200 rpm) is shown in Figure 2B. It is observed that the ratio of the intensity of the two LSPR peaks is lower than that in the case of the sample prepared at 1600 rpm stirring speed. This indicates that the conversion of the quasi-spheres and cubes into nanorods increases as the stirring speed increases. When the stirring speed is lowered to 400 rpm, only one LSPR peak is observed corresponding to the quasi-spherical nanoparticles. This suggests that at these low stirring speeds none of the mother clusters are distorted sufficiently to form nanorod seeds.

To further examine the role that temperature and stirring speeds play in the AgNRs synthesis, we varied a number of conditions: (1) We examined the effect of the stirring speed by carrying the synthesis at 175 °C at three different stirring speeds (400, 1200, and 1600 rpm) for the same reaction time. Figure 3A−C shows the SEM images of silver nanoparticles formed at the same initial concentrations and temperature of 175 °C but at different stirring speeds. It is clear that as the stirring speed increases the yield of the AgNRs (that is, the amount of rods that are formed relative to the amount of isotropic-in-shape, i.e., non-nanorod-shaped, particles, e.g., spheres, cubes, and prisms). Only a small yield of rods is obtained at stirring speeds below 400 rpm (Figure 3A). Increasing the stirring speed to values exceeding 1600 rpm (up to 2500 rpm) did not have an effect on the yield of silver nanorod formation. (2) To examine the need for high temperature during the AgNRs synthesis, the temperature was decreased to 165 °C, but the stirring speed was kept high (1600 rpm). Under these conditions, the majority of the resulting nanoparticles possesses quasi-spherical and cubic shapes, and no rods were formed. (3) The effect of growth time on the yield of AgNRs was monitored by comparing the yield of AgNRs in samples taken at different reduction (growth) times from the batches prepared at different stirring speeds (1600, 1200, and 400 rpm) at 175 °C. Figure S1 shows the SEM images of AgNRs prepared at 175 °C and at stirring speed of 1200 rpm. As in the case of the AgNRs prepared at 1600 rpm and at 175 °C, the length of the AgNRs was found to increase

dx.doi.org/10.1021/nl402305n | *Nano Lett.* 2013, 13, 4739−4745

as the growth period is increased. However, no significant change in the percentage yield of the AgNRs was observed. For the silver nanoparticles prepared at 400 rpm and 175 °C, the quasi-spherical particles formed increased with the reduction time.

Possible Mechanism of the Symmetry Breaking of the Silver Nanocrystals. Colloidal synthesis of nanoparticles by the chemical methods proceeds via formation of small seeds (mother clusters, or nuclei), which grow into nanoparticles by selective growth on the nanocrystalline facets. Thus in describing the growth of the nanoparticles, one needs to consider jointly the core composition (Ag in our system) and the binding affinities of the capping material (here, PVP) to the various exposed facets. Thus the shape of the resulting nanoparticles depends mainly on the shape of the seed and the type of capping material used in the synthesis. Two common techniques are used in the colloidal chemical method. In the seed-mediated technique, the seeds are formed in a separate solution before transfer to the growth solution. In the other method the seeds are formed in situ (as is the case here), followed by subsequent growth steps. It is well-known that the {110} facet of Ag has higher surface energy than that of the {111} and {100} facets and therefore weaker atomic Ag bonding.[6] The surface energies of crystals having these facets decrease in the order: {110} 0.953 eV > {100} 0.653 eV > {111} 0.553 eV.[28] The normal reduction of silver ions leads to the formation of stable faceted particles, with overall isotropic shapes (that is, quasi-spherical), exposing the low surface energy {111} and {100} facets.

To obtain anisotropic shapes, the symmetry of the growth process of the nanoparticle should be perturbed either through induced anisotropic growth[10,29] or through creation of twinning defects.[5] The question raised by our observations of anisotropic growth as a result of high-rate stirring pertains to the physical processes that underlie the development of the anisotropic shapes of silver nanoparticles prepared under stirring conditions. To understand the mechanism by which high speed stirring leads to the formation of AgNRs, we analyze first the shape of the seeds. When stirring is stopped subsequent to the formation of the seeds (the appearance of the red color), the synthesis of the AgNRs does not cease.

HR-TEM was used to study the structure of the seeds formed. Figure 4A shows the HR-TEM image of seed nanoparticles isolated during the synthesis of AgNRs at a stirring speed of 1600 rpm. The seed appears to be pentatwinned.[19] From the lattice resolved image in Figure 4B, the lattice *d*-spacing was found to be 0.234 and 0.200 nm which correspond to the {111} and {100} facets, respectively.[30,31] The lattice *d*-spacing in the twin boundary is 0.234 nm which corresponds to the {111} facet. Early detailed theoretical investigations have indeed shown[32] that pentatwinned decahedral small metal particles exhibit enhanced stability, with the internal decahedral (5-fold symmetry) stress being counterbalanced by the presence of the low energy {111} facets on the outer (exposed) boundaries (interfacing with the growth solution). It is pertinent to note here that for silver nanoparticles prepared at low stirring speed (400 rpm) we find a quasi-spherical structure with multiple {111} and {100} facets resulting from symmetrical growth of a single crystalline seed (see Figure S3).

The following text discusses a plausible theoretical scenario for the formation of the pentatwinned seed at high stirring speed. The first step of the colloidal nanoparticle synthesis entails the formation of small clusters, with each growing into a nanoparticle seed. These small solid crystalline clusters are surrounded by a surface (physical) adsorption layer, namely, a region with a thickness of ∼1 nm (a few molecular diameters) envisioned by Volmer as early as in 1922.[33] This thin boundary region forms the interface between the solid crystallite and the solution, and its properties differ greatly from a slice of bulk solution having a comparable width.[23] It is in this thin layer that the silver ions are desolvated, reduced, and diffuse to the adsorption sites on the surface of the cluster where they are incorporated into the growing nanocrystal. Additionally this interfacial region plays a role in transport of solvent molecules and of heat (generated by the energy relaxation accompanying the accommodation of the metal atoms and their binding to the lattice sites of the growing crystallite) away from the growth interface. The above surface adsorption region is surrounded by a volume diffusion boundary region of much larger width than the adsorption region. In this region a concentration gradient of silver ions is established, which decreases on moving away from the surface of the cluster toward the bulk of the solution. If diffusion through this relatively wide boundary layer is the rate-limiting step in the growth of the crystal, even gentle stirring will tend to increase the growth rate as had been originally postulated by Nernst,[21] with the width, δ, of the diffusion layer decreasing as $\delta \sim u^{-1/2}$ where u is the liquid flow velocity past the crystals' solid facet.[23]

To understand the effect of stirring on the rate and in particular the anisotropic symmetry of the growing nanocrystal, we focus on the way that liquid flow relative to the growing solid crystallite affects the aforementioned interfacial adsorption region proximal to the surface of the growing nanocrystallite. The pioneering work of Volmer[33] and his contemporaries provided the foundations for understanding crystal growth processes, but it lacked microscopic detail. Early molecular dynamics simulations of the growth of crystals from a liquid onto a solid surface (liquid-phase epitaxy, LPE) have revealed formation of a region exhibiting density oscillations in the liquid, at the interface with the solid surface (see refs 34−38). Such a liquid-layering boundary (LLB) region, which we identify with the aforementioned Volmer interfacial region, forms under equilibrium conditions, as well as under non-equilibrium ones (that is during LPE, see below). Typically, 4−6 liquid layers are formed, and the amplitudes of the density oscillations associated with these liquid layers decay to the liquid bulk density value over a distance of about 1 nm along the normal to the solid facet-to-liquid interface. These layers are characterized by close to liquid-like intralayer structure (parallel to the solid facet) and by anisotropic atomic diffusivities which are smaller in the direction perpendicular to the interface, and in the layers themselves (i.e., parallel to the solid −liquid interface) they take intermediate values, that is, smaller than those in the bulk liquid and larger than found in the solid. Furthermore, the degree and extent of the above interfacial liquid-layering, as well as the morphology of the solid−liquid interface, have been found to depend on the exposed solid surface (i.e., the (h,k,l) Miller indices), with increased corrugation and roughness leading to reduced layering propensity.[39]

It has been suggested early on[34,35] that the above-mentioned interfacial liquid-layering process may be viewed as the initial kinetic step in the LPE growth process. As the degree of order in that liquid layer increases (that is, as the region closer to the solid surface, or parts of that region, transform into an added

dx.doi.org/10.1021/nl402305n | *Nano Lett.* 2013, 13, 4739−4745

epitaxially grown solid layer), the LLB moves one layer up further into the liquid, with the formation of an added liquid-layered region located further away from the newly established solid–liquid interface. In this way the width (~1 nm) of the LLB region maintains throughout the LPE growth process. As aforementioned, less-corrugated facets [that is, (111) and (100) facets of fcc metals] exhibit a larger propensity for development of the LLB region than facets with higher corrugations, for example, (110) and facets with higher Miller indices.

The above formation of the LLB region, and the processes occurring in this proximal interfacial zone (in particular, energy relaxation and accommodation of liquid metal atoms at sites of the solid surface, diffusion of solvent molecules away from that zone, and transport of heat generated by the LPE relaxation and crystallization processes), may be influenced by external fields. Here we focus on liquid flow associated with mechanical stirring of the liquid. The stirring motion introduces relative shear flow on facets oriented in a direction parallel to the flow direction of the liquid past the solid–liquid interface. This shear flow, and the shear stress that it exerts on the molecules in the LLB region, affect the propensity of density ordering in the liquid (that is reducing liquid-layering).

In particular, recent molecular dynamics (MD) simulations[40] (see the Supporting Information) have revealed that the onset of sufficiently fast shear liquid flow parallel to the plane of a crystalline facet, induced by high-rate stirring during liquid-phase epitaxial growth, obliterates and inhibits formation of the LLB region in the liquid proximal to that facet, resulting in arrested growth of the crystal on that facet. Since in our system the initial seed exposes (111) and (100) surfaces (see Figure 4A), the effect of stirring is predicted to transform the growth preferentially to the (110) direction. This effect of stirring on the growth kinetics, together with the stronger binding of the PVP capping material to the (100) facets of silver, would result in the effective growth of silver nanorods with high aspect ratios, with the long axis of the grown AgNR in the (110) direction, capped by (111) facets.

Selected results from our MD simulations are shown in the theoretical section of the Supporting Information. In these simulations we explored nanocrystalline growth, for a stationary seed, as well as under the influence of stirring at various velocities (that is applied rotation of the seed relative to the surrounding liquid). Our simulations illustrate (see Figures S5 and S6) the onset of anisotropic growth of the nanocrystallite above a critical rotational velocity, V_{rc}, resulting in a rod-shaped nanocrystal with an aspect ratio $\lambda = (c/\langle a \rangle) > 1$, for example, $\lambda = 2.6$ (see Figure S6 for $V_r = 2.2 \times 10^{-3}\ \tau^{-1}$, where τ is the characteristic time unit, estimated to be 0.2 ps for silver, see SI); λ is the ratio between the long (c, $\langle 110 \rangle$) axis (which coincides with the rotation axis, z, of the seed) and the average of the transverse dimension ($\langle a \rangle$) of the nanocrystal's cross-section normal to the $\langle 110 \rangle$ direction. Interestingly at even higher rotational velocities (e.g., $V_r = 2.64 \times 10^{-3}\ \tau^{-1}$), growth of the seed is arrested, and no growth is recorded. This arrested growth regime corresponds to rotational-shear-flow-induced motions of impinging (liquid) Ag atoms adsorbing on the facets of the solid silver seed crystallite, which occur at a faster rate than the rate of energy relaxation and accommodation required for incorporation of the liquid Ag atoms into the growing crystallite—under these conditions the rotational-flow-induced frustration of the structure and processes occurring in the nanometer scale interfacial liquid boundary layer (the aforementioned LLB) is large enough so as to stop the growth. For rotational velocity $V_r < V_{rc}$ the shape of the growing crystallite is found to remain approximately spherical (see the evolution of the shape of the growing crystallite recorded at selected times during the simulation, shown in Figure S5 for $V_r = 0.44 \times 10^{-3}\ \tau^{-1}$). In agreement with the experimental results, we found in our simulations that the growth velocity decreases as the rotational (stirring) velocity increases.

Our experiments confirm the above expectations. The pentatwinned seed, prepared at high stirring speed, grows into a AgNR [with the long axis in the (110) direction] whose HR-TEM image is shown in Figure 4C. Detailed analysis of a lattice resolved images of the AgNR revealed that the tip of the nanorod is composed of {111} facet (Figure 4D). To get further insight into the crystal structure, another AgNR was imaged by HR-TEM, and the results are shown in Figure 4E. The HR-TEM images of the two AgNRs are not identical, which is attributed to the presence of multiple faces for the AgNR. The enlarged HR-TEM image in Figure 4F reveals that the side boundaries of the AgNR are composed of {100} facets,

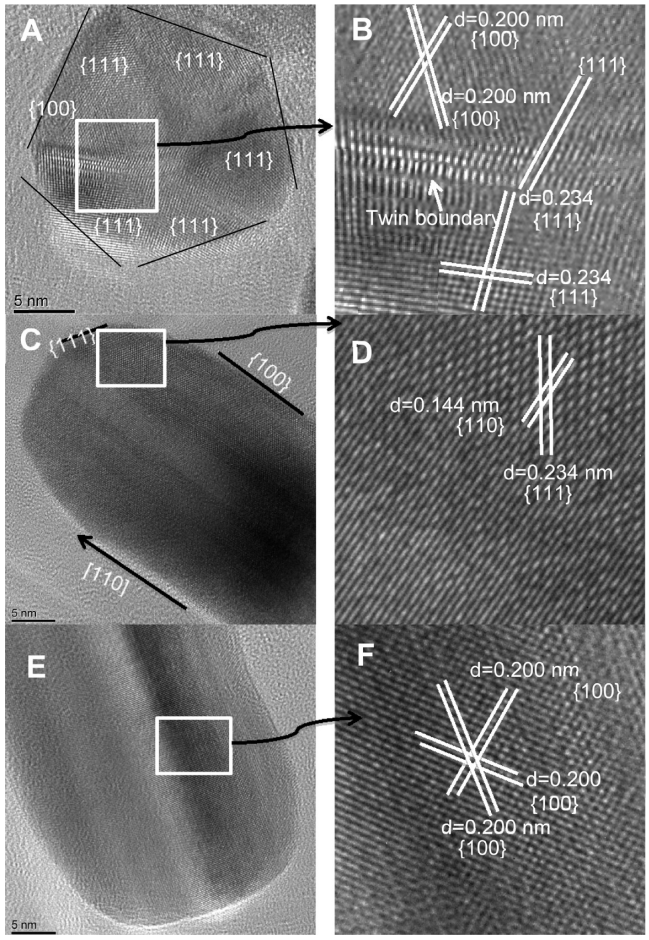

Figure 4. HR-TEM and structural analysis of the silver seeds and silver nanorods formed at high stirring speed and high temperatures: HR-TEM of (A) AgNR pentatwinned seed. (B) Lattice-resolved TEM image of AgNRs seed, the lattice d-spacing corresponding to the known {111} and {100}, the twin sites has {111} facets. (C) HR-TEM image of a tip of an individual AgNR. (D) Lattice resolved TEM image of part of AgNR the lattice d-spacing shows the presence of {111} and {110}. (E) HR-TEM image of an individual AgNR from the side view. (F) Lattice-resolved TEM image of AgNR from the side, the lattice d-spacing shows the presence of the {100} facet.

dx.doi.org/10.1021/nl402305n | Nano Lett. 2013, 13, 4739–4745

which, as aforementioned are preferentially stabilized by the PVP capping polymer. Based on this information, the growth mechanism of the AgNRs may be described as follows: The twin sites are the most active part on the surface of pentatwinned seed. Silver atoms are deposited on these sites. Since the twin sites have neighboring {111} facets (meeting at the twining boundary), the pentatwinned silver seed grows on the {111} facets. This causes the growth of the AgNR along the [110] direction, with the tip capped by (111) facets and the side walls of the nanorod exposing (100) facets.

Conclusion. A new method for bringing about symmetry breaking, requisite for the growth of silver nanoparticles during the polyol reduction of silver ions to form the hard-to-synthesize silver nanorods, is demonstrated. This method is based on high-speed stirring at high temperatures during the reduction of silver ions to make the silver "seed cluster". At high rotation speeds (1600 rpm) and high temperatures, we were able to inhibit the natural formation of symmetric, low surface energy clusters, that lead to generation of sphere- or cube-shaped nanoparticles. Instead, the (high energy) pentatwinned seeds formed under the influence of high-frequency stirring resulting in the growth of rod-shaped nanoparticles.

When high-frequency stirring is maintained throughout the entire growth process, nanorods with a narrow aspect ratio distribution are generated. On the other hand, when stirring is stopped shortly after the formation of the seeds, the nanorods that form are characterized by a broad aspect ratio distribution, while the width of the nanorods is almost the same as that of the initially formed seed cluster (see Figure S4 in the SI). The aspect ratio of the silver nanorods prepared by this new seedless synthetic method can be easily increased by increasing the reaction time. The wavelength of the longitudinal plasmon band of the silver nanorods prepared by this method can be increased from 500 to 1000 nm by increasing the reaction time past the seed formation stage. The width of the nanorods can be enlarged only by increasing of the initial concentration of the silver ions (during the seed formation period under high frequency stirring). As the stirring speed decreases at high temperatures, the yield of nanorods decreases, and below a certain threshold of stirring speeds no nanorods are formed resulting in production of symmetric nanoparticles such as quasi-spheres, cubes, and prisms.

The symmetry-breaking effect of stirring on the growth of silver nanoparticles is discussed in the framework of a microscopic description of the liquid-to-solid interface between the growing silver cluster and the surrounding solution. Molecular dynamics simulations reveal formation of a thin (~1 nm, i.e., a few atomic diameters thin) liquid-layered boundary (LLB) region at the interface between the crystalline facet and the liquid, serving as an embryonic kinetic stage of crystal growth from the liquid onto the solid facet. Formation of the LLB, identified here with the well-known Volmer adsorption region[33] where reduction of the silver ions, desolvation, diffusion, and eventual incorporation onto the crystalline facet lattice occurs, has been found to be highly frustrated by the action of sufficiently fast stirring-induced shear liquid flow on facets oriented parallel to the flow. Consequently, we predict that high-frequency stirring can kinetically inhibit growth on the (low-energy) facets of the pentatwinned cluster seed. Together with preferential binding of the PVP polymer to the silver (100) facets, growth proceeds in the (110) direction, resulting in symmetry breaking, and yielding (see Figure S6 in the SI), in agreement with our observations, silver nanorods extended in the (110) direction, capped at the ends by (111) facets, and exposing (100) facets on the side walls.

■ ASSOCIATED CONTENT

Ⓢ Supporting Information

Experimental procedure for synthesis of silver nanoparticles. SEM images of AgNRs of different aspect ratios prepared at stirring speed of 1200 rpm (Figure S1). Table S1 is the longitudinal LSPR peak position of AgNRs with different aspect ratios. Figure S2 is the linear relationship between the length of the AgNRs and the growth time of the silver pentatwinned seed. Figure S3 is the HR-TEM image of quasi-spherical silver nanoparticles. Figure S4 is the SEM images of AgNRs prepared under the same chemical and physical conditions as in Figure 1 except the stirring is stopped shortly after the formation of the seeds. The theoretical section gives a detailed description of our MD simulations of crystalline growth for variable velocities of applied rotations (stirring) of the initial crystalline seed relative to the surrounding liquid. It is shown that while no stirring, as well as slow applied rotational velocities, result in a quasi-spherical grown crystallite (Figure S5), elongated rod-like crystallites are grown for stirring velocities above a critical value (Figure S6). This material is available free of charge via the Internet at http://pubs.acs.org.

■ AUTHOR INFORMATION

Corresponding Author

*E-mail: melsayed@gatech.edu.

Notes

The authors declare no competing financial interest.

■ ACKNOWLEDGMENTS

The authors would like to thank Mr. Justin Bordley for helping with taking the TEM. The work of M.A.M. and M.A.E. was supported by the Office of Basic Energy Sciences of the US. .Department of Energy under Contract No. DE-FG02-97-ER 14799, while the work of U.L. was supported by the same agency under a contract No. FG05-86ER45234, and J.G. was supported by a grant from the Air Force Office of Scientific Research.

■ REFERENCES

(1) Kreibig, U.; Vollmer, M. *Optical Properties of Metal Clusters*; Springer Series in Materials Science 25; Springer: New York, 1995; p 532.

(2) Ahmadi, T. S.; Wang, Z. L.; Green, T. C.; Henglein, A.; El-Sayed, M. A. *Science* **1996**, *272*, 1924−1926.

(3) Freund, P. L.; Spiro, M. *J. Phys. Chem.* **1985**, *89*, 1074−1077.

(4) Turkevich, J.; Stevenson, P. C.; Hillier, J. *Discuss. Faraday Soc.* **1951**, *11*, 55−75.

(5) Wang, Z. L.; Mohamed, M. B.; Link, S.; El-Sayed, M. A. *Surf. Sci.* **1999**, *440*, 809−814.

(6) Wang, Z. L.; Gao, R. P.; Nikoobakht, B.; El-Sayed, M. A. *J. Phys. Chem. B* **2000**, *104*, 5417−5420.

(7) Sun, Y. G.; Xia, Y. N. *Science* **2002**, *298*, 2176−2179.

(8) Millstone, J. E.; Hurst, S. J.; Metraux, G. S.; Cutler, J. I.; Mirkin, C. A. *Small* **2009**, *5*, 646−664.

(9) Jin, R. C.; Cao, Y. W.; Mirkin, C. A.; Kelly, K. L.; Schatz, G. C.; Zheng, J. G. *Science* **2001**, *294*, 1901−1903.

(10) Jana, N. R.; Gearheart, L.; Murphy, C. J. *J. Phys. Chem. B* **2001**, *105*, 4065−4067.

(11) Pietrobon, B.; McEachran, M.; Kitaev, V. *ACS Nano* **2009**, *3*, 21−26.

(12) Jana, N. R.; Gearheart, L.; Murphy, C. J. *Chem. Commun.* **2001**, 617−618.
(13) Tao, A.; Kim, F.; Hess, C.; Goldberger, J.; He, R. R.; Sun, Y. G.; Xia, Y. N.; Yang, P. D. *Nano Lett.* **2003**, *3*, 1229−1233.
(14) Zhang, J.; Langille, M. R.; Mirkin, C. A. *Nano Lett.* **2011**, *11*, 2495−2498.
(15) Nehl, C. L.; Liao, H. W.; Hafner, J. H. *Nano Lett.* **2006**, *6*, 683−688.
(16) Mahmoud, M. A.; Tabor, C. E.; El-Sayed, M. A.; Ding, Y.; Wang, Z. L. *J. Am. Chem. Soc.* **2008**, *130*, 4590−4591.
(17) Wang, Z. L.; Kang, Z. C. *Functional and Smart Materials-Structure Evaluation and Structure Analysis*; Plenum Press: New York, 1998; Chapter 6.
(18) Wiley, B.; Sun, Y. G.; Mayers, B.; Xia, Y. N. *Chem.—Eur. J.* **2005**, *11*, 454−463.
(19) Xia, X. H.; Xia, Y. N. *Nano Lett.* **2012**, *12*, 6038−6042.
(20) Wiley, B.; Herricks, T.; Sun, Y. G.; Xia, Y. N. *Nano Lett.* **2004**, *4*, 1733−1739.
(21) Nernst, W. *Z. Phys. Chem.* **1904**, *47*, 52−55.
(22) Carlsson, A. E. *Growth and Perfection of Crystals*; John Wiley & Sons: New York, 1958; p 421.
(23) Scheel, H. J.; Elwell, D. *J. Electrochem. Soc.* **1973**, *120*, 818−824.
(24) Valenzuela, R.; Fuentes, M. C.; Parra, C.; Baeza, J.; Duran, N.; Sharma, S. K.; Knobel, M.; Freer, J. *J. Alloys Compd.* **2009**, *488*, 227−231.
(25) Garcia, M. A.; Bouzas, V.; Carmona, N. *Mater. Chem. Phys.* **2011**, *127*, 446−450.
(26) Carbo-Argibay, E.; Rodriguez-Gonzalez, B.; Pastoriza-Santos, I.; Perez-Juste, J.; Liz-Marzan, L. M. *Nanoscale* **2010**, *2*, 2377−2383.
(27) Link, S.; Mohamed, M. B.; El-Sayed, M. A. *J. Phys. Chem. B* **1999**, *103*, 3073−3077.
(28) Vitos, L.; Ruban, A. V.; Skriver, H. L.; Kollar, J. *Surf. Sci.* **1998**, *411*, 186−202.
(29) Nikoobakht, B.; El-Sayed, M. A. *Chem. Mater.* **2003**, *15*, 1957−1962.
(30) Nepijko, S. A.; Ievlev, D. N.; Schulze, W.; Urban, J.; Ertl, G. *ChemPhysChem* **2000**, *1*, 140−142.
(31) Hofmeister, H.; Nepijko, S. A.; Ievlev, D. N.; Schulze, W.; Ertl, G. *J. Cryst. Growth* **2002**, *234*, 773−781.
(32) Cleveland, C. L.; Landman, U. *J. Chem. Phys.* **1991**, *94*, 7376−7396.
(33) Volmer, M. *Z. Phys. Chem* **1922**, *102*, 267−275.
(34) Cleveland, C. L.; Landman, U.; Brown, C. S. *Phys. Rev. Lett.* **1980**, *45*, 2032−2035.
(35) Landman, U.; Cleveland, C. L.; Brown, C. S.; Barnett, R. N. Molecular dynamics of surfaces and epitaxial solidification. *Nonlinear Phenomena at Phase Transitions and Instabilities*; Riste, T., Ed.; Plenum: New York, 1981.
(36) Landman, U.; Luedtke, W. D.; Barnett, R. N.; Cleveland, C. L.; Ribarsky, M. W.; Arnold, E.; Ramesh, S.; Baumgart, H.; Martinez, A.; Khan, B. *Phys. Rev. Lett.* **1986**, *56*, 155−158.
(37) Landman, U.; Luedtke, W. D.; Ribarsky, M. W.; Barnett, R. N.; Cleveland, C. L. *Phys. Rev. B* **1988**, *37*, 4637−4646.
(38) Luedtke, W. D.; Landman, U.; Ribarsky, M. W.; Barnett, R. N.; Cleveland, C. L. *Phys. Rev. B* **1988**, *37*, 4647−4655.
(39) Gao, J.; Luedtke, W. D.; Landman, U. *Tribol. Lett.* **2000**, *9*, 3−13.
(40) Gao, J.; Landman, U. *Unpublished*, 2013.